ACS OMEGA

Open Access

http://pubs.acs.org/journal/acsodf

Article

Influence of Polyphosphate on the Mineralization Balance of Tooth Enamel

Jing Ru,[#] Xiaochen Xu,[#] Yuxuan Cheng, Nan Luo, Shuo Tan, Xi Chen,* Feng Chen,* and Bing-Qiang Lu*

Cite This: *ACS Omega* 2025, 10, 10162−10172

Read Online

ACCESS | Metrics & More | Article Recommendations | Supporting Information

ABSTRACT: Dental minerals are in an equilibrium state of demineralization and remineralization, which can be disrupted by pathogenic bacteria to cause dental caries. While the inorganic polymer polyphosphate (polyP) is ubiquitous in living organisms and is also widely involved in mineralization regulations, its specific influence on the mineralization balance of teeth remains unclear. As a concept-and-proof study, the effects of polyP on the demineralization and remineralization of teeth are investigated on dental enamel (the highly mineralized outer covering tissue of teeth) from the perspective of mineralization balance. We found that a high concentration (containing 1.0−20 mM P element, comparable to and higher than the free phosphate ions in body fluids) of polyP has the capability to demineralize enamel in the aqueous solution, yet this effect is absent in the simulated biological environments including simulated body fluid and MEM (α-minimum essential medium) solutions. More importantly, polyP with a very low concentration (containing ≥5.0 μM P) is able to inhibit enamel mineralization significantly. This suggests that polyP could impact the mineralization balance of enamel by preferentially inhibiting the remineralization process, thereby disrupting the equilibrium necessary for maintaining enamel health.

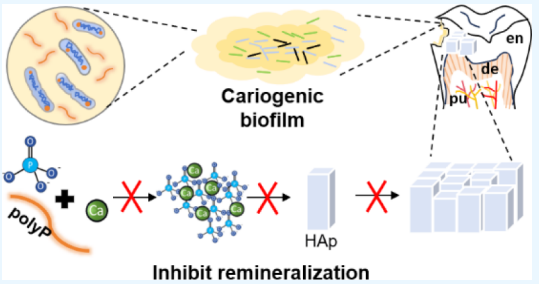

1. INTRODUCTION

Dental caries is a prevalent and intricate chronic disease that is caused primarily by cariogenic bacteria encompassing *Streptococcus mutans* (*S. mutans*), *Lactobacillus acidophilus* (*L. acidophilus*), and various actinomyces within the ecologically abnormal microbiome. Upon colonization on teeth and the subsequent formation of cariogenic biofilm,[1] these bacteria yield acids including lactic, acetic, butyric, and propionic acids, which in turn lower the local pH, leading to the demineralization of tooth surfaces.[2−5] While the precise pathogenic mechanism of caries remains incomplete, organic acids yielded by the microorganisms are incontrovertibly the principal factor that chemically demineralizes the teeth.[6] Besides acids, other factors that influence the local mineralization balance (demineralization vs. remineralization), including reduced salivary flow,[7] saliva composition,[8] chelation by organics,[9−11] etc., have also been proposed.

Despite the focus on organic biomolecules that influence the balance of mineralization processes, the role of one inorganic polymer-polyphosphates (polyPs) in caries has been seemingly overlooked, although it is essential in various bacteria and other life forms (both prokaryotes and eukaryotes).[12] Possessing a linear molecular polymer structure composed of orthophosphate residues that are linked by high-energy phosphoanhydride bonds, polyP is important for various cellular functions, including bacterial virulence,[13−15] biofilm formation,[15,16] quorum sensing,[15] competitive fitness in the environment,[17] microbial stress responses,[14,18,19] and survival during the stationary phase,[18,20] storage and supply of phosphorus,[21] and energy supply.[22,23] It is also believed that polyP plays a role in the regulation of mineralization, e.g., resisting the mineralization and providing phosphate for mineralization via its hydrolysis.[24] However, as an effective mineralization regulator, its interplay with the mineralization-associated disease—dental caries—remains unclear. Previous reports have identified the presence of polyP, along with genes and enzymes associated with its metabolism in *L. acidophilus* species.[25] One study also proposed that some pathogenic bacteria can accumulate polyphosphate (polyP), lower the saturation state of ions in the surrounding liquid, and increase the solubility of dental minerals, which may be linked to cariogenesis.[26] These discoveries provided insights into the potential role of polyP in the cariogenic process. However, there is a lack of experimental evidence supporting the demineralizing capability of polyP, and more importantly, its impact on the remineralization process has yet to be explored.

Received: October 5, 2024
Revised: December 12, 2024
Accepted: February 20, 2025
Published: March 4, 2025

Herein, in order to further elucidate the link between polyP and caries from the perspective of mineralization balance, we investigated the demineralization and remineralization of teeth on dental enamel (the highly mineralized covering tissue of teeth) in the presence of polyP. Accordingly, two possibilities were explored: on one hand, as implied by the report,[26] polyP could chelate Ca^{2+} ions, resulting in a demineralization of the enamel; on the other hand, the presence of polyP may inhibit remineralization, a mineral deposition or restoration process of the enamel. Based on this hypothesis, this work made a concept-and-proof study. First, we confirmed the presence of polyP in *L. acidophilus* (a common oral pathogen) and cariogenic biofilms samples. Subsequently, we investigated the specific influences of polyP in demineralization and remineralization across different environments. The results found that polyP could disrupt the mineralization balance by preferentially inhibiting the remineralization process, instead of directly enhancing demineralization, suggesting a possible pathway for its involvement in the pathogenesis of dental caries.

2. MATERIALS AND METHODS

2.1. Materials and Reagents. Polyphosphate salts with three different chain lengths were used for this study: sodium hexametaphosphate with an average chain length of 6 phosphate (Pi) units was purchased from Sigma-Aldrich, Germany (denoted as $polyP_1$); sodium polyphosphate with an average chain length of 22 phosphate (Pi) units was purchased from Aladdin Biochemical Technology Company, China (denoted as $polyP_2$); ammonium polyphosphate with an average chain length of about 2800 phosphate (Pi) units was purchased from Aladdin Biochemical Technology Company, China (denoted as $polyP_3$). *Lactobacillus acidophilus* (*L. acidophilus*, ATCC4356) was obtained from the China General Microbiological Culture Collection Center (CGMCC). α-Minimum essential medium (MEM) was purchased from Biosharp. Simulated Body Fluid (SBF) was purchased from Fuzhou Phygene Biotech Co., Ltd. $CaCl_2{\cdot}2H_2O$ was obtained from Sigma-Aldrich, Germany. Isothiazolinone (2-methyl-4-isothiazoline-3-one, MIT) was obtained from Rhawn Chemical Reagent Company.

All chemicals were obtained without further purification. In this paper, the concentration of polyP in each solution is recorded as that of the phosphorus element (also equals to the concentration of phosphate residues).

2.2. Detection of PolyP in Pathogenic Bacteria. Confocal laser scanning microscopy (CLSM, Nikon N-SIM, Japan) was applied to visualize polyP in pathogenic bacteria *Lactobacillus acidophilus* (*L. acidophilus*, ATCC4356, CGMCC). They were cultured in MRS broth (Sigma-Aldrich) culture media at 37 °C for 24 h to logarithmic growth. Then, the solution was centrifuged at 8000 rpm for 3 min to obtain the sedimented bacteria after discarding the supernatant. The bacteria were washed three times with phosphate buffer solution (PBS) and suspended in 0.1% DAPI (4′,6-diamidino-2-phenylindole) solution for uniform staining. The stained bacteria were transferred to a CLSM dish, and the fluorescence signals were recorded by a CLSM. According to the literature, DAPI bonds to DNA and polyP in bacteria to form DNA−DAPI and polyP−DAPI complexes, respectively, which both have fluorescence effects; however, their emissions can be distinguished based on the different emission maxima.[26] In the fluorescence spectra of DNA−DAPI and polyP−DAPI, excitation (Ex) and emission (Em) wavelengths are Ex/Em: 345/455 nm for the DNA−DAPI complex and Ex/Em: 415/550 nm for the polyP−DAPI complex. In CLSM observation, upon an excitation wavelength of 345 nm, DNA−DAPI displayed a blue color in filter path 1 (emission wavelength from 410 to 480 nm); upon an excitation wavelength of 415 nm, polyP−DAPI exhibited a green color in filter path 2 (emission wavelength from 480 to 550 nm).

2.3. Detection of PolyP in Cariogenic Biofilms. The collection of human cariogenic biofilms was reviewed and approved by the Ethics Committee of Shanghai Ninth People's Hospital (Approval No.: SH9H-2022-T413-1). Samples of human cariogenic biofilms were collected from the carious tooth surfaces of patients with dental caries using a sterile applying brush head, which was in accordance with standard cariogenic biofilm collection procedures at Shanghai Ninth People's Hospital, and patients' consent was obtained before collection. Participants fasted for 1 h before sampling and did not brush their teeth on the morning of the sampling day.

The detection methods for polyP in cariogenic biofilm samples were similar to those in bacteria. Briefly, the clinically collected cariogenic biofilm samples were immediately fixed with paraformaldehyde for 15 min and then suspended in 0.1% DAPI (4′,6-diamidino-2-phenylindole) solution for staining. The stained biofilms were transferred onto a dish, and the fluorescence signals were recorded by a CLSM. The operating parameters including the wavelength settings of the CLSM were consistent with those in Section 2.2.

2.4. Preparation of Dental Enamel Blocks. The enamel blocks prepared from human teeth were used for studies of tooth surface demineralization and remineralization. Human third molars without caries and other conditions were extracted for clinical reasons (insufficient eruption space or impaction) following standard procedures for extraction at the Shanghai Ninth People's Hospital and handled with permission from the Ethics Committee of Shanghai Ninth People's Hospital (Approval No.: SH9H-2024-T351-1). The collected teeth were cleaned with deionized water and temporarily stored in 75% ethanol for further use. The dental crowns were cut with a low-speed wheel diamond saw (Model 971, JIAODA, China) to obtain the enamel blocks (3 × 3 × 5 mm), which were then polished with waterproof silicon carbide paper (600, 1000, 2000, and 5000 grit in sequence). The samples were cleaned with ethanol, soaked in ultrasound for 30 s, and dried at room temperature. On each sample, half side was coated with 50 μL nail varnish (YX01, YULYNA, China) to cover it with an acid-resistant layer after drying, and this side was denoted as the nontreatment half side (self-control).[27] The other half side was exposed as the treatment side for demineralization or remineralization. At the end of the experiments, the enamel blocks were placed in acetone (99.5%) for 24 h to remove the nail varnish for characterization.

2.5. Demineralization of Enamel Blocks by PolyP. PolyPs were dissolved in water, SBF, and MEM to prepare three different polyP solutions (denoted as polyP-water, polyP-SBF, and polyP-MEM, respectively) for this study. The polyP-water interaction, with minimal influences from external factors, can reveal the basic interaction between polyP and enamel. SBF is a buffered solution of mineral ions with concentrations comparable to those of body fluids; MEM is a buffered solution of organic nutrients and mineral ions for the culture of cells. Thus, these two solutions were applied to simulate the complex biological environment. Three polyPs

https://doi.org/10.1021/acsomega.4c09093
ACS Omega 2025, 10, 10162−10172

with different chain lengths were used: $polyP_1$, $polyP_2$, and $polyP_3$.

First, the polyP-water solutions ($polyP_1$, $polyP_2$, $polyP_3$) with pH 7.4 and concentrations of 1.0, 5.0, 10, and 20 mM were prepared. Prior to the experiment, half side of each enamel block was covered with an acid-resistant nail varnish as the nontreatment half side (self-control), and the other half side was exposed. Then, the enamel blocks, with their polished surfaces upward, were incubated in the above polyP solutions at 37 °C for demineralization, whereby the exposed sides were demineralized but the nail varnish-coated sides were protected. The polyP solution was replaced daily with fresh one, which was kept for 3 days. In addition, we investigated the long-term demineralization effects of $polyP_2$ solution on enamel blocks by replacing fresh $polyP_2$ solutions of low concentrations (1.0, 0.5, 0.1 mM) daily for 14 consecutive days. The resulting samples were characterized after washing with water, removing the nail varnish with acetone (99.5%), and drying at room temperature.

In order to detect the released Ca during enamel demineralization in the polyP-water solution, the enamel blocks were soaked in the 5 mM polyP-water solution (pH 7.4) for demineralization. After 24 h, the supernatant was collected. Then, the content of Ca in it was measured (see the details in Section 2.8).

The experimental procedures for demineralization in polyP-SBF and polyP-MEM were the same as those in polyP-water ($polyP_2$ was selected as representative). polyP-SBF and polyP-MEM with polyP concentrations of 1.0, 5.0, 10, and 20 mM were used to study the influence of polyP on enamel demineralization.

2.6. Mineralization Inhibition of Enamel Blocks by PolyP. PolyPs were dissolved in MEM and SBF to prepare polyP solutions denoted as polyP-MEM and polyP-SBF for this study.

Like in body fluids and saliva, the cell culture medium MEM contains both inorganic salt ions (Ca^{2+}, PO_4^{3+}, Na^+, K^+, Cl^-, etc.) and organics (glucides, amino acids, ribonucleosides, etc.) which resemble the compositions of saliva and body fluids, making it an ideal solution to mimic the environment in the mouth. In this study, a common cell culture medium (α-MEM, Biosharp) was used as the mineralization fluid. PolyPs were introduced into the fluids, resulting in the final concentration of each polyP at 0, 2.0, 5.0, and 10 μM, respectively. Prior to use, 30 μL of $CaCl_2$ (1.0 M) solution was added into 10 mL of the original MEM solution to increase the supersaturation for triggering the mineralization, and fungicide MIT was introduced at the concentration of 100 μg/mL for sterilization.[28,29]

Self-comparisons were also applied for the evaluation of enamel mineralization, where half side of each enamel block was covered by an acid-resistant nail varnish as the nontreatment half side (self-control), and the other half side was exposed. Then, the enamel blocks, with their polished surfaces facing upward were incubated in 10 mL of the above fluids at 37 °C for 3 days (replacing the fluid with fresh one daily), whereby the exposed sides were mineralized, but the nail varnish-coated sides were protected. The inhibitory effect of polyP on mineralization was observed on the resulting enamel blocks after washing with water, removing the nail varnish with acetone (99.5%), and drying at room temperature.

Given that mineral formation has the potential to induce variations in solution turbidity, an investigation into the mineralization process across different mineralization fluids was conducted by employing a turbidimeter (LH-Z10A, Zhejiang, China) to measure the changes in turbidity exhibited by these fluids. The precipitates during turbidity change were further characterized by alizarin red staining and transmission electron microscopy (see the details in Section 2.8).

In order to analyze precipitated minerals during remineralization, 10 mL polyP-MEM solutions with different concentrations of $polyP_2$ were prepared, followed by adding 30 μL of $CaCl_2$ (1.0 M) solution to initiate the precipitation. After 24 h, the polyP-MEM solutions were centrifuged to separate the supernatant and precipitates, which were then analyzed separately.

The mineralization inhibition experimental procedure in polyP-SBF is the same as that in polyP-MEM ($polyP_2$ was selected as a representative).

2.7. The Interaction between PolyP and Calcium Ions. The interaction between polyP and Ca^{2+} was investigated by comparing the electrical potentials of calcium ions in specific solutions ($CaCl_2$ solution or MEM solution) with and without polyP. An ion meter (PXSJ-216F, Lei-ci, Shanghai) equipped with a calcium ion electrode (PCa-1-01, Lei-ci, Shanghai) was used to detect the electrical potentials of calcium ions. Prior to the use of the calcium ion electrode, it was rinsed with distilled water and soaked in a 0.001 mol/L $CaCl_2$ solution for 2 h to activate it, thereby achieving better sensitivity and response capability.

Detection in a $CaCl_2$ solution: first, 50 mL of a 1.5 mM $CaCl_2$ solution was prepared (the Ca^{2+} concentration is close to that in healthy human body fluids). Then, the $polyP_2$ solution (100.0 mM) was added to it to make the concentrations of $polyP_2$ reach 10 μM, 10^2 μM, 10^3 μM, 5×10^4 μM, and 10^4 μM, respectively. Meanwhile, the calcium ion electrical potentials were recorded.

Detection in MEM solution: similarly, the $polyP_2$ solution (100.0 mM) was dropped into 50 mL of MEM to make the concentrations of $polyP_2$ reach 10 μM, 10^2 μM, 10^3 μM, 5×10^4 μM, and 10^4 μM, respectively, and the corresponding changes in calcium ion electrical potentials were recorded as well.

2.8. Characterizations. *2.8.1. Scanning Electron Microscopy.* Scanning electron microscopy (SEM, FEI, Nova Nano 450, USA) was used to observe the morphology of the enamel block surfaces after washing with water, removing the nail varnish with acetone, and drying at room temperature. After the specimens were dried, they were mounted onto the SEM sample holder with conductive tape. The specimens were sputtered with a thin gold layer in a vacuum sputtering chamber for 60 s at 10 mA to enhance conductivity. For SEM imaging, the acceleration voltage was 3.00 kV for a balance of image resolution and damage reduction, and the working distance was adjusted to 5.5 mm. Images of the secondary electrons were captured for observation.

2.8.2. Transmission Electron Microscope. Samples were immediately centrifuged at 10,000 rpm for 1 min, and the supernatant was discarded and washed with water and anhydrous ethanol at least three times. The samples were dispersed in ethanol and characterized using a transmission electron microscope (TEM, JEM-2100F, JEOL, Japan) to obtain the morphology and selected area electron diffraction (SAED) pattern.

2.8.3. Fourier Transformed Infrared Spectroscopy. Fourier transform infrared spectroscopy (FTIR) analysis on tooth enamel blocks was performed in attenuated total reflectance

https://doi.org/10.1021/acsomega.4c09093
ACS Omega 2025, 10, 10162−10172

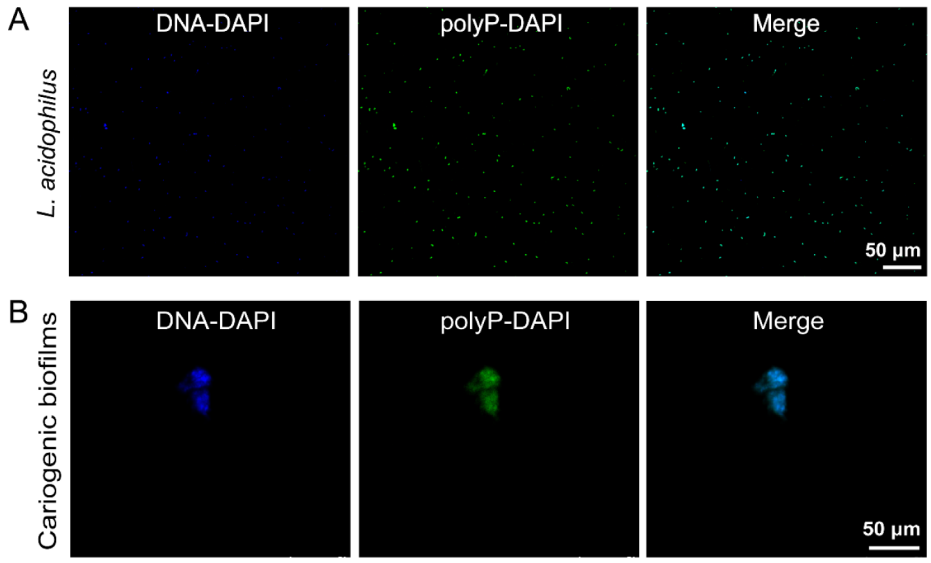

Figure 1. Detection of polyP in caries pathogens and clinical caries plaque samples. (A) CLSM images of *L. acidophilus* bacteria stained with DAPI (scale bar: 50 μm). (B) CLSM images of cariogenic biofilm samples stained with DAPI (scale bar: 50 μm). The blue and green images correspond to fluorescent signals of the DNA−DAPI and polyP−DAPI complexes, respectively.

(ATR) mode using an FTIR spectroscope (Nicolet iS20, Thermo Fisher Scientific). Dried enamel specimens were placed on the ATR crystal, and FTIR spectra (4000−400 cm^{-1}) were collected with 32 scans. After data acquisition, the spectra were smoothed using a Savitzky−Golay filter with a polynomial degree of 2. Characteristic vibration bands corresponding to specific chemical bonds or groups were identified and analyzed following the spectra of hydroxyapatite in literature.[30]

2.8.4. Surface Hardness Test. The hardness of tooth enamel blocks was measured by a Vickers microhardness tester (Tukon2500). Control group: enamel pieces soaked in deionized water for 3 days; experimental groups: enamel blocks demineralized by 5.0 mM polyP solutions ($polyP_1$, $polyP_2$, $polyP_3$) for 3 days. The surface hardness of each group was assessed three times, and each sample was indented three times by using a load of 0.490 N applied for 15 s. The score for each specimen was calculated as the average of the three results.

2.8.5. Measurement of the Concentrations of Ca and P in Solutions. After the sample collection, HCl (100 μL, 3M) was added to 5 mL of the supernatant sample to avoid any sediments. The concentration of Ca and P in each supernatant was tested by an inductively coupled plasma emission spectrometer (ICP-OES, iCAP 7600, Thermo, USA). Custom Assurance Standard solutions (XNEF-54C, SPEX CertiPrep) were used as the standard substance. For the measurement of supernatants collected in demineralization experiments, standard solutions were diluted to concentration gradients of 0, 4, 8, 12, 16, and 20 ppm to calibrate the Ca concentration. For the measurement of supernatants collected in remineralization experiments, standard solutions were diluted to concentration gradients of 0, 50, 100, 150, 200, and 250 ppm to calibrate the Ca concentration or to 0, 5, 10, 15, 20, 25, and 30 ppm for calibration of P concentration.

2.8.6. Alizarin red Staining. The polyP-MEM with different concentrations of $polyP_2$ was cultured 24-well plates at 37 °C. After 4 h and 8 h, the solution was collected and centrifuged at 10000 rpm for 2 min. The precipitation was collected, washed with deionized water twice, and stained with Alizarin red (0.2% Alizarin red S solution). The stained precipitate was added to 1 ml deionized water, mixed with a pipette gun, dispersed into 96-well plates, and immediately observed under an optical microscope.

2.9. Statistical Analysis. Each experiment was repeated at least three times. Under the same conditions, three samples were included in each repetition. All measurements were presented as the mean ± SD. Statistical analysis was conducted via GraphPad Prism 8.0. Statistical analyses were conducted using one-way ANOVA and Tukey's HSD tests. A value of $p < 0.05$ was considered as statistically significant.

3. RESULTS

3.1. Detection of PolyP in Caries Pathogens and Cariogenic Biofilms. As an exploration of the association between polyP and dental caries, it is essential to detect polyP in related pathogens. Herein, we confirmed the presence of polyP in *L. acidophilus* experimentally following the previous study.[26] The bacteria were stained with DAPI to label the internal polyP via the formation of a polyP−DAPI complex (along with the formation of a DNA−DAPI complex), which can be identified by confocal laser scanning microscopy (CLSM).[31] Indeed, as shown in Figure 1A, the bacteria exhibited blue and green signals in filter path 1 (emission wavelength from 410 to 480 nm) and filter path 2 (emission wavelength from 480 to 550 nm), respectively, strongly indicating the presence of polyP in them.

We also confirmed the existence of polyP in cariogenic biofilms, whose formation is a critical step toward caries. The detection methods including wavelength settings of CLSM for polyP in cariogenic biofilm samples are similar to those for bacteria. The cariogenic biofilm samples were collected from the carious teeth of patients, stained with DAPI, and observed with a CLSM again. The DNA−DAPI complex in the biofilms also shows blue fluorescence, along with the green of a polyP−DAPI complex, as shown in Figure 1B. Therefore, both in free bacteria and biofilm, polyP has been identified, which is consistent with the previous report.[26]

https://doi.org/10.1021/acsomega.4c09093
ACS Omega 2025, 10, 10162−10172

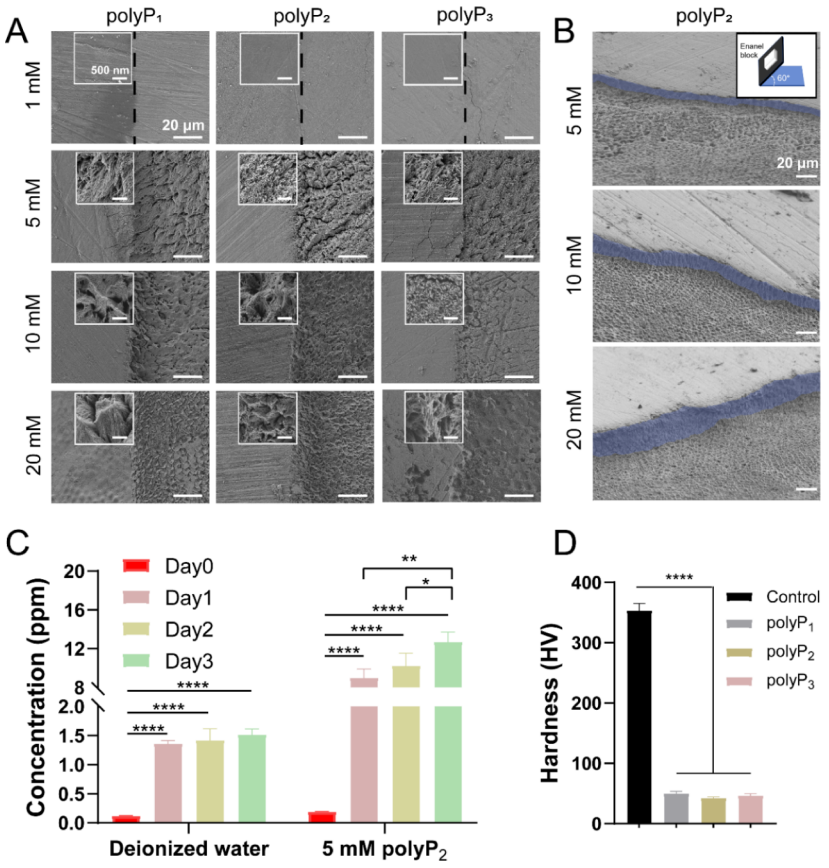

Figure 2. Effect of polyP on enamel demineralization in polyP-water. (A) SEM images of enamel blocks demineralized in polyP-water with 1.0 5.0, 10, and 20 mM polyP (scale bars: 20 μm). Insets: magnified SEM images of the treated sides (scale bars: 500 nm). (B) SEM images of the demineralization depth of enamel blocks viewed at a tilt of 60° (scale bars: 20 μm). (C) Ca concentrations in the supernatants after soaking enamel blocks in deionized water and 5.0 mM $polyP_2$ solution for different days (day 0: original Ca concentration in deionized water). (D) Average Vickers hardness of the tooth enamel blocks after being soaked in deionized water and 5.0 mM polyP solutions for 3 days. All data are presented as mean ± SD from at least three independent biological replicates. Statistical analyses were conducted using one-way ANOVA and Tukey's HSD tests. * means $p < 0.05$; ** means $p < 0.01$; *** means $p < 0.001$; **** means $p < 0.0001$.

3.2. Demineralization of Enamel Blocks by PolyP.

Enamel samples were cultured in three polyP solutions (polyP-water, polyP-MEM, and polyP-SBF) to investigate their demineralization behavior. First, enamel demineralization in polyP/water was investigated. As shown in Figures 2A and S1, on the enamel blocks cultured in polyP-water solutions ($polyP_1$, $polyP_2$, $polyP_3$) at a concentration of 1.0 mM for 3 days, or lower concentrations for longer incubation duration (14 days), there is no distinct morphological difference between the nontreated area and the treated area of each sample, which remains smooth without visible mineral loss (Figure 2A). Thus, at such a low concentration, the polyP solution does not corrode tooth enamel significantly. When the concentrations of polyPs are raised to 5.0−20 mM, distinct mineral loss occurs on the surface of the treated area, showing the fish scale-like pattern due to the uneven demineralization (Figure 2A), which resemble that of acid-etched enamel.[32] Moreover, the enamel samples were tilted at 60° for side-view observations. As shown in Figure 2B, the increase in polyP concentration leads to a progression in the corrosion depth and thus more mineral loss. Subsequently, attenuated total reflectance-Fourier transform infrared spectroscopy (ATR-FTIR) was used to analyze the demineralized enamel surfaces. On the spectra (Figure S2), the characteristic bands of hydroxyapatite (the main component of enamel) are broadened significantly compared to those of the blank samples (enamel blocks without treatments). Therefore, in addition to mineral loss, demineralization caused by polyP may have also damaged the crystallinity of the remaining hydroxyapatite crystals.

To corroborate that the morphological change on the enamel surface is attributed to the demineralization process, instead of ion rearrangement by the reaction between polyP and hydroxyapatite, concentration changes of Ca in the demineralization solutions were measured. After soaking the enamel blocks in deionized water (blank) and 5.0 mM polyP−water solutions ($polyP_1$, $polyP_2$, $polyP_3$) for different days (replacing the solutions with fresh ones daily), the supernatants were tested using ICP-OES (Figure 2C). It shows that, at all of the measured time points, the concentration of Ca in polyP solutions is significantly higher than that in deionized water, revealing the promoted dissolution of enamel minerals by polyPs; i.e., a demineralization process occurs.

In addition, we measured the Vickers hardness of enamel blocks after demineralization in polyP solutions for 3 days. As demonstrated in Figure 2D, the hardness of the resulting enamel decreases from the original 353.8 HV to much lower values, i.e., less than 50.4 HV, indicating that the demineralization by polyP has significantly weakened the mechanical properties of the enamel. This can be explained by

https://doi.org/10.1021/acsomega.4c09093
ACS Omega 2025, 10, 10162−10172

the porous and fish scale-like surface morphology and reduced crystallinity of the surface hydroxyapatite crystals shown above.

Second, demineralization was investigated in two solutions that simulate complex biological environments: polyP-SBF and polyP-MEM. In contrast to the pronounced effect observed in polyP-water, enamels in these two solutions are much more intact (Figures 3 and S3). In Figure 3, enamel surfaces remain

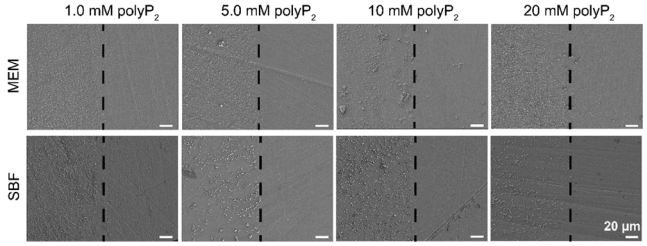

Figure 3. SEM images of enamel blocks after 3 days of immersion in polyP-SBF and polyP-MEM with $polyP_2$ concentrations of 1.0, 5.0, 10, and 20 mM, respectively. Dashed line in each image: boundary of the nontreatment (left) and the treatment (right) sides. Due to the very weak demineralization of the treated sides, totally removing the nail varnish would lead to the difficulty in distinguishing the boundary of the treatment/nontreatment sides; thus, only partial of the nail varnishing was dissolved in acetone with granular residues on the left sides. Scale bars: 20 μm.

smooth on the treated sides in both polyP-SBF and polyP-MEM after 3 days, despite the varying polyP concentrations ranging from 1.0 to 20 mM. Such weak performances in demineralization remain even after a longer term of 14 days (Figure S3). This indicates that the diverse ions in polyP-SBF and polyP-MEM have significantly compromised the demineralization capacity of polyP, suggesting its potential limitations in complex biological environments (e.g., saliva).

3.3. Mineralization Inhibition by PolyP. As body fluids and saliva are supersaturated with ions of Ca^{2+} and phosphate with respect to the solubility of HAP,[33] the demineralized teeth undergo a certain level of recovery in these fluids, i.e., a process known as remineralization (reversal to mineralization). In this context, apart from demineralization, inhibition of remineralization is also associated with the equilibrium of tooth minerals. Therefore, as a typical mineralization inhibitor,[34−36] the influence of polyP on the remineralization of teeth was studied in this work. In brief, varied concentrations of polyP solutions were introduced into the supersaturated mineralization fluids (MEM with excess $CaCl_2$) to prepare the polyP-MEM; then it was used to culture the enamel blocks; afterward, the mineralization layer in the treated areas (with the nail varnish-covered area as the self-control) of the enamel blocks was observed (Figure 4).

It is found that enamel blocks in the fluid without polyP (blank sample, 0 μM polyP in polyP-MEM) undergo obvious mineralization in the treated areas, forming a thick mineralization layer according to the SEM images (Figure 4B). With 2.0 μM polyP in polyP-MEM, the mineralization layer exhibits no significant change in comparison to the blank, indicating a poor mineralization inhibition effect of polyP at such a low concentration (Figure 4C). As the polyP concentration rises to 5.0 μM, while there remains a mineralization layer, it is noticeably thinned compared to the blank (Figure 4D). Further elevating the polyP concentration to 10 μM, the mineralization layer is almost invisible, indicating a significant inhibitory effect of polyP on mineralization at such a concentration (Figure 4E).

Further insights into the change in the polyP-MEM during incubation were explored (Figure 4F−H). In the absence of the mineralization inhibitor polyP, the reaction between Ca^{2+} and phosphate in the fluid results in distinct turbidity and mineral precipitation after 24 h. With the addition of polyP, turbidity and precipitation are distinctly reduced with 5.0 μM polyP in polyP-MEM. However, once the polyP concentration in the fluid reaches 10 μM, turbidity and precipitation do not occur. Turbidity evolution in the fluids was quantitatively analyzed with a turbidimeter to confirm the observations above. The initial turbidity of the fluid without polyP is measured to be 1.6 NTU, consistent with its transparent state. The value escalates to 74.8 NTU after 24 h, attributed to the formation of mineral precipitation. However, in the presence of polyPs, the turbidity of the fluids after 24 h displays significantly lower values than those of blank samples, and they decrease with the rise of polyP concentration (Figure 4F−H).

In order to elucidate more details of the inhibition effect of polyP, the evolution of the polyP-MEM with different concentrations of $polyP_2$ (but in the absence of enamel blocks) and the formed minerals was measured (Figure 5). Tracking the turbidity change process, we find that precipitation in the fluids with $polyP_2$ at the concentration of 0−5.0 μM all begins after 3 h and progresses over time. However, the turbidity of the fluids with 10 μM $polyP_2$ remains static due to a much stronger mineralization inhibition effect, agreeing with the observed mineralization inhibition as above. Besides, we centrifuged the four solutions at 10,000 rpm to remove the precipitates, collected the supernatant, and measured the residual Ca and P in it by ICP-OES. In Figure 5B, the concentrations of Ca and P in the fluid without polyP are 189.1 and 30.4 ppm, but drop to 136.8 and 11.4 ppm after 24 h, respectively. However, in the presence of $polyP_2$, such a concentration drop is significantly inhibited. Especially, at 10 μM $polyP_2$, the concentrations of Ca and P in the supernatant remain very close to those in the original fluid, which is consistent with the few precipitates formed in the solution.

As a characterization of the precipitates, the polyP-MEM with different concentrations of $polyP_2$ was cultured in a 24-well plate, and then the resulting precipitates were stained by 0.2% alizarin red S solution (marking the calcium salts) for microscope observation. As displayed in Figure 5C, the amounts of alizarin red-marked calcium sediments (with red color) decrease significantly upon increasing the content of $polyP_2$, which is consistent with the turbidity change in the fluids. The component of the precipitates was further confirmed using a transmission electron microscope (TEM), by which the particles show a selected area electron diffraction (SAED) pattern of HAP (Figure 5D). These all prove that the precipitates are HAP, and its formation in the fluids can be inhibited by polyP.

The inhibition of polyP against mineralization was also investigated in another buffered solution of minerals—polyP-SBF (Figure 6). Analogous to observations in polyP-MEM, the inhibitory effect is enhanced with increasing polyP concentration in polyP-SBF, and 10 μM polyP leads to nearly invisible mineral precipitation on the enamels. This implies that the mineralization inhibition effect of polyP is robust in different conditions and is concentration-dependent.

https://doi.org/10.1021/acsomega.4c09093
ACS Omega 2025, 10, 10162−10172

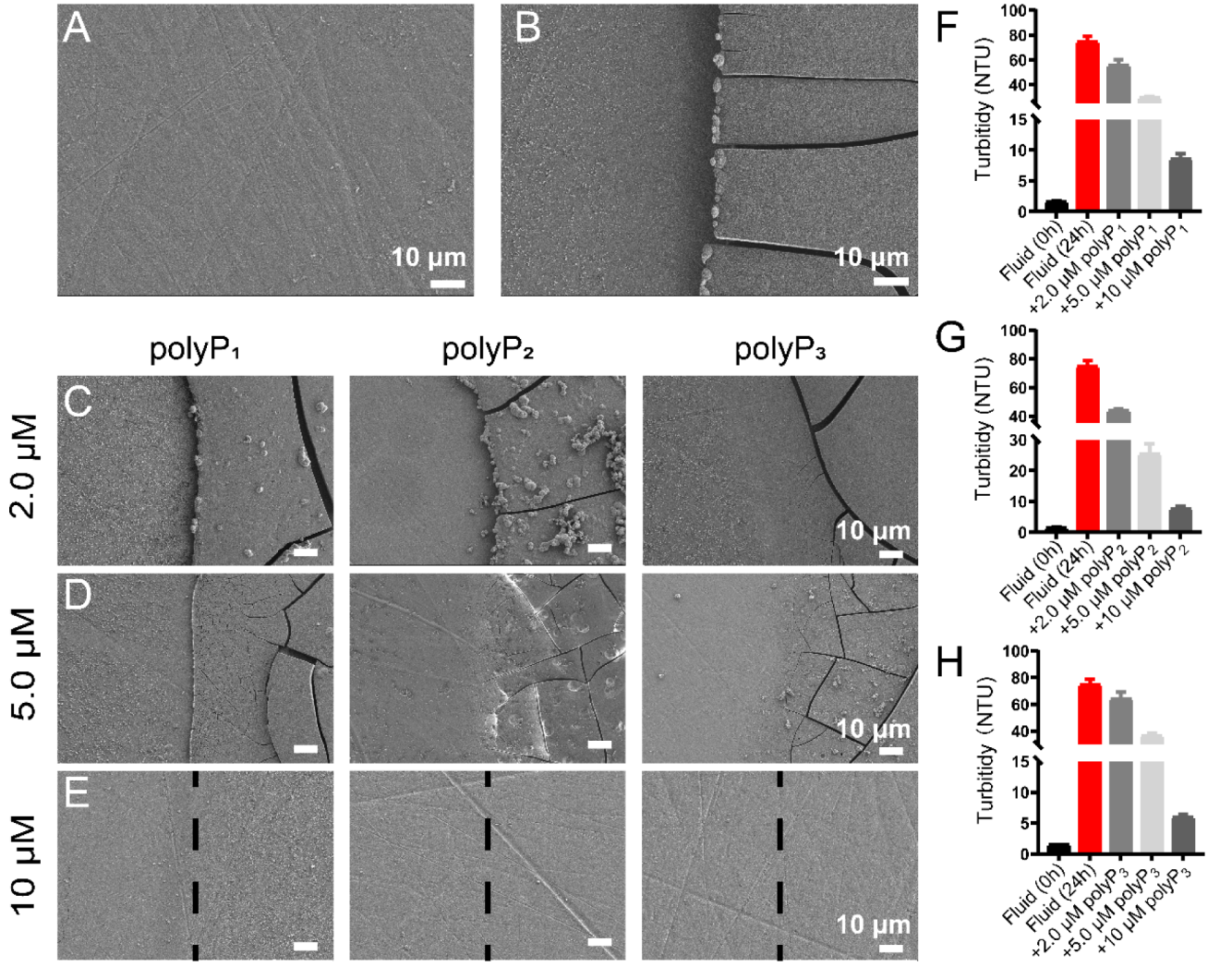

Figure 4. Inhibition of mineralization by polyP in the polyP-MEM. (A, B) SEM images of the original tooth enamel block before (A) and after remineralization for 24 h (B) in the fluids. (C–E) SEM images of enamel blocks after mineralization in polyP-MEM with 2.0 μM (C), 5.0 μM (D), and 10 μM (E) polyPs. Left side of each image (A–E): the nontreatment side; right side of each image: treated side. Dashed line in each image (E): boundary of the nontreatment (left) and treatment (right) sides (scale bars: 10 μm). (F–H) Turbidity values of polyP-MEM with different concentrations of $polyP_1$ (F), $polyP_2$ (G), and $PolyP_3$ (H) after incubating enamel blocks for 24 h.

3.4. Interaction between PolyP and Ca^{2+}. The demineralization and remineralization caused by polyP should be linked with the interplay between polyP and Ca^{2+}, a relationship that can be illuminated by observing the variations in Ca^{2+} activity in Ca^{2+} solutions, both in the presence and absence of polyP. As Ca^{2+} activity is positively correlated with Ca^{2+} potential in solutions,[37] we monitored the Ca^{2+} potential changes in 1.5 mM $CaCl_2$ solution and MEM upon adding $polyP_2$.

Initially, the Ca^{2+} potential in 1.5 mM $CaCl_2$ solution without $polyP_2$ is −219.8 mV. Upon adding $polyP_2$ to this solution, a gradual decline in Ca^{2+} potential is observed, culminating in a value of −325.0 mV at a polyP concentration of 10 mM. A comparable trend is noted in MEM solutions: the initial Ca^{2+} potential in MEM is −226.4 mV, which decreases to −254.9 mV at a polyP concentration of 10 mM. This decrease in the Ca^{2+} potential serves as an indicator of reduced free Ca^{2+} activity in the solution, implying an increased binding of Ca^{2+} to $polyP_2$. This decrease in Ca^{2+} potential serves as an indicator of reduced Ca^{2+} activity in the solution, implying an increased binding of Ca^{2+} to $polyP_2$.

4. DISCUSSION

It has been well established that dental mineral is in an equilibrium state of demineralization and remineralization,[38] where the former loses the mineral and the latter accumulates or restores it.[7] The disruption of the balance between demineralization and remineralization can be affected by various physiological factors, including the biomolecules secreted by bacteria. It is generally believed that cariogenic bacteria, via the generation of organic acids, cause overwhelming demineralization and lead to dental caries. However, the interplay between caries and other nonacid molecules originating from bacteria, e.g., polyP, is much less studied, although a recent study proposed a mechanism regarding demineralization by it.[26] As an essential inorganic biopolymer in various bacteria and mineralization-involved molecules, it is reasonable to speculate that polyP could influence caries in the processes of demineralization or remineralization.

As a concept-and-proof study based on such speculation, we first confirmed the existence of polyP in cariogenic bacteria. Common cariogenic bacteria include *S. mutans*, *L. acidophilus*, etc.,[26,39] and *S. mutans* acts in caries development predom-

https://doi.org/10.1021/acsomega.4c09093
ACS Omega 2025, 10, 10162−10172

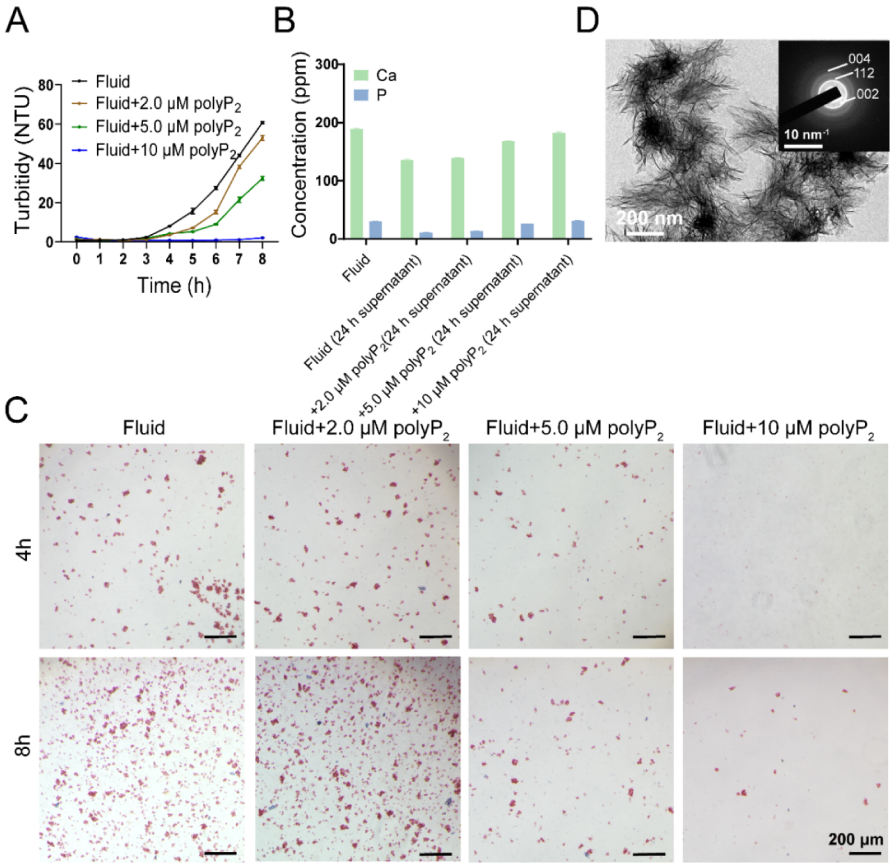

Figure 5. Mineralization Inhibition in polyP-MEM. (A) Turbidity change over time in the supersaturated mineralization fluids with $polyP_2$ of different concentrations (0, 2.0, 5.0, and 10 μM). (B) The element content of Ca and P in supernatant determined by ICP-OES after removing the precipitates by centrifugation. (C) Optical microscopic images of the formed precipitates with alizarin red staining. Scale bars: 200 μm. (D) TEM image and SAED pattern (inset) of the precipitates obtained by centrifugation of supersaturated mineralization fluids after incubating for 24 h.

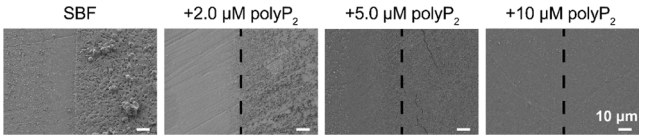

Figure 6. SEM images of enamel blocks after mineralization in polyP-SBF with 2.0, 5.0, and 10 μM of $polyP_2$. Dashed line in each image: boundary of the nontreatment (left) and treatment (right) sides. Scale bars: 10 μm.

inantly, but studies have shown that *S. mutans* lacks the genes associated with the key enzymes for polyP formation.[26] Therefore, we primarily verified the presence of polyP in *L. acidophilus*. Following the literature, we observed the fluorescent signal of polyP in the normal cariogenic bacteria *L. acidophilus* with CLSM after DAPI staining. Subsequently, we found that polyP is abundant in cariogenic biofilms of patients with dental caries. Therefore, polyP may be positively correlated with the occurrence and development of caries.

On the other hand, we investigated the capacity of polyP in promoting dental demineralization using the enamel blocks as the *in vitro* model. When immersing the enamel blocks in polyP-water solutions, distinct demineralization can be observed at concentrations of ≥5.0 mM. Such conclusions are evidenced by the distinct mineral loss on the enamel surface and the increased concentration of Ca in the solution. As a notable consequence, such a demineralization reduces the hardness of enamel to a large extent, which would severely impair the function of the enamel.

Previous studies suggested that polyP derived from bacteria may lead to changes in the saturation state of the surrounding oral environment and thus promote demineralization.[26] While that report did not observe the demineralization of enamel by polyP experimentally, we here do confirm such an effect in the polyP-water (Figure 2). In addition, we also corroborate that the presence of the polyP does reduce Ca activity in both the $CaCl_2$ solution and MEM cell culture medium (Figure 7). However, it should be noted that the effective concentration of polyP for demineralization investigated here (>1.0 mM) is at a

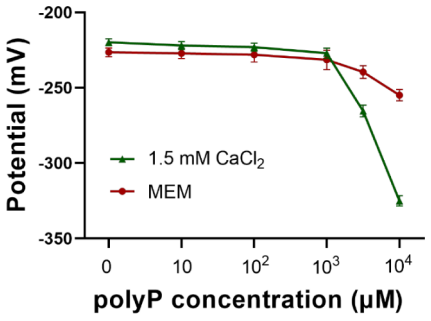

Figure 7. Ca ion potential detected by the calcium ion selective electrode in 1.5 mM $CaCl_2$ solution and MEM with the addition of $polyP_2$.

https://doi.org/10.1021/acsomega.4c09093
ACS Omega 2025, 10, 10162−10172

very high level and is even comparable to that of phosphate in saliva and human body fluid,[40,41] which greatly compromises its effectiveness, although the precise measurement of the polyP concentration in the cariogenic biofilms is challenging due to technical limitations.

While the demineralization effect of polyP in pure water is distinct, demonstrating a fundamental capacity of polyP that in simulated biological environments is greatly attenuated. The solutions polyP-SBF and polyP-MEM with even 20 mM polyP fail to cause significant mineral loss on enamels. Given that polyP-SBF and polyP-MEM are both buffered solutions of mineral ions, and MEM contains additional organic nutrients, it is reasonable that these ions and organics act to passivate the polyP. In these solutions, polyP could referentially chelate with the free cations, e.g., Ca^{2+} and Mg^{2+} in solutions, rather than those on the enamel surfaces, which thereby drastically reduces its demineralizing potential. Besides, mineral ions of polyP-SBF and polyP-MEM are in the supersaturated state, offering sufficient cations for the chelation to polyP before transitioning into the undersaturation state, thus further limiting its interaction with enamel surface minerals.

Finally, we studied the influence of polyP in inhibiting the remineralization on the enamel blocks in polyP-MEM and polyP-SBF. Due to the high supersaturation in the fluids, a layer of minerals could deposit on the surface of enamel blocks in the absence of mineralization inhibitors including polyP. Based on this property, the inhibitory effect of polyP was evaluated by observing the change in mineral deposition when introducing polyP into the fluids. It turns out that at a very low concentration of 5.0 μM, the mineralization of enamel can be dramatically inhibited, resulting in much less mineral deposition. Furthermore, at a higher concentration of 10 μM, mineral deposition is mostly prevented on the enamel. Such a strong inhibitory effect was further corroborated by measuring the turbidity of the supersaturated mineralization fluids (with or without polyPs) after incubation in polyP-MEM: the turbidity of the solution progression can be significantly reduced by polyP. Also, the precipitates are determined to be HAP according to the characterizations by alizarin red staining, TEM, and SAED.

Compared to the high concentration of polyP required for demineralization (>1.0 mM) in polyP-water, the concentration needed for mineralization inhibition ($\geq$5.0 μM) is much lower in all tested fluids. In addition, this effective concentration is also lower than other reported normal nucleation inhibitors, e.g., pyrophosphate,[42] PAA,[43] and citrate.[44] Usually, mineralization progresses via two critical steps: nucleation and crystallization. While it has been proposed that polyP can prevent crystallization and crystal growth[45,46] by chelating Ca^{2+} and occupying the crystallization site of hydroxyapatite, the significant reduction of mineral formation by polyP in this work can be attributed to its inhibition against nucleation which directly determines the mineral formation instead of its crystallinity. Despite chelating Ca^{2+}, the highly effective performance of polyP in nucleation inhibition, like other inhibitors, could be a result of its direct influence on the nucleation process, e.g., the stability and transformation of nucleus or prenucleation species,[47,48] which is worthy of future study.

For the different polyPs with varied molecular weights, we failed to observe significant differences in their performances during demineralization and remineralization inhibition. Typically, the appropriate concentrations for demineralization or inhibition of mineralization are largely consistent across the different molecular weights of polyPs. In addition, the influences of all tested polyPs on enamel surface morphology, mechanical strength, release of ions, mineralized layers, etc., are very similar to each other.

As one of the initial studies exploring the relationship between polyP and dental caries, this research indeed harbors several limitations, which should be resolved in the following studies. First, the etiology of dental caries is intricate, being the cooperation of numerous chemical and biological processes. This study primarily focuses on the perspective of mineralization balance with less discussion on the in-depth role of polyP among the biological factors. Particularly, its secretion and transport by bacteria, as well as interactions with other biological molecules, remain elusive. Second, an adequate method for detecting the extracellular concentration of polyP, particularly within the biofilm of bacteria, was not established. Thus, while the capability of polyP in mineralization inhibition was observed even at the micromolar concentration level, a definitive conclusion regarding its role in caries cannot yet be established. Lastly, considering the actual complex process of dental caries, a longer duration of the experiments and different chain lengths of polyPs in different conditions should be considered for the study.

Nevertheless, in addition to the development in fundamental aspects, the findings in this work might be helpful to clinicians as well. They could potentially use such knowledge to better understand the factors influencing caries and consider alternative preventive or treatment strategies. For example, in patients at high risk of caries, awareness of the role of polyPs would prompt more vigilant monitoring the concentration of polyP in the mouth; besides, they can explore adjunctive therapies counteracting the inhibitory effect, e.g., hydrolysis of polyP or prevention of polyP formation in cariogenic bacteria and biofilms by specific agents.

5. CONCLUSION

In conclusion, after concept-and-proof insights into the role of polyP in the progression of dental caries from the perspective of mineralization balance, this study unveils a potential pathway through which polyP may facilitate caries development. Essentially, polyP demonstrates a capacity to disrupt the mineralization balance in simulated biological environments preferentially by inhibiting remineralization, rather than enhancing demineralization. This characteristic of polyP does not support the prior reports that attributed its effect on caries to the induction of demineralization via lowering saliva saturation. Instead, it elucidates an alternative mechanism underlying the polyP-associated caries progression, specifically its inhibition of remineralization.

■ ASSOCIATED CONTENT

Supporting Information

The Supporting Information is available free of charge at https://pubs.acs.org/doi/10.1021/acsomega.4c09093

SEM images of enamel blocks after being soaked in polyP-water with $polyP_2$ of low concentration for 14 days (Figure S1); ATR-FTIR spectra of demineralized enamel block surfaces (Figure S2); SEM images of enamel blocks after 14 days of immersion in polyP-SBF and polyP-MEM with polyP2 concentrations in the range of 0−10 mM (Figure S3) (PDF)

https://doi.org/10.1021/acsomega.4c09093
ACS Omega 2025, 10, 10162−10172

AUTHOR INFORMATION

Corresponding Authors

Xi Chen − *Department of Preventive Dentistry, Shanghai Ninth People's Hospital, Shanghai Jiao Tong University School of Medicine, Shanghai 200011, P. R. China*; Email: chenx1853@sh9hospital.org.cn

Feng Chen − *Suzhou First People's Hospital, School of Medicine, Anhui University of Science and Technology, Huainan, Anhui 232000, P. R. China; Center for Orthopaedic Science and Translational Medicine, Department of Orthopedic, Spinal Pain Research Institute, Shanghai Tenth People's Hospital, School of Medicine, Tongji University, Shanghai 200072, P. R. China; Shanghai Key Laboratory of Craniomaxillofacial Development and Diseases, Shanghai Stomatological Hospital & School of Stomatology, Fudan University, Shanghai 201102, P.R. China*; orcid.org/0000-0002-1162-1684; Email: fchen@tongji.edu.cn

Bing-Qiang Lu − *Center for Orthopaedic Science and Translational Medicine, Department of Orthopedic, Spinal Pain Research Institute, Shanghai Tenth People's Hospital, School of Medicine, Tongji University, Shanghai 200072, P. R. China*; orcid.org/0000-0002-7027-0351; Email: bqlu@tongji.edu.cn

Authors

Jing Ru − *Suzhou First People's Hospital, School of Medicine, Anhui University of Science and Technology, Huainan, Anhui 232000, P. R. China*

Xiaochen Xu − *Department of Preventive Dentistry, Shanghai Ninth People's Hospital, Shanghai Jiao Tong University School of Medicine, Shanghai 200011, P. R. China*

Yuxuan Cheng − *Yuncheng Center for Disease Control and Prevention, Yuncheng, Shanxi 044300, P. R. China*

Nan Luo − *Department of Preventive Dentistry, Shanghai Ninth People's Hospital, Shanghai Jiao Tong University School of Medicine, Shanghai 200011, P. R. China*

Shuo Tan − *Center for Orthopaedic Science and Translational Medicine, Department of Orthopedic, Spinal Pain Research Institute, Shanghai Tenth People's Hospital, School of Medicine, Tongji University, Shanghai 200072, P. R. China*

Complete contact information is available at: https://pubs.acs.org/10.1021/acsomega.4c09093

Author Contributions

#Jing Ru and Xiaochen Xu contributed equally.

Notes

The authors declare no competing financial interest.

ACKNOWLEDGMENTS

This work was financially supported by the National Key R&D Program of China (2022YFE0123500), the National Natural Science Foundation of China (52272304, 31771081, 82370941), the Science and Technology Commission of Shanghai Municipality (21ZR1449700, 22S31903300), the Science and Technology Bureau of Suzhou City (SZKJXM202318), and the Open Project of Shanghai Key Laboratory of Magnetic Resonance in East China Normal University (SKMR2023A02).

REFERENCES

(1) Krzyściak, W.; Jurczak, A.; Kościelniak, D.; Bystrowska, B.; Skalniak, A. The virulence of Streptococcus mutans and the ability to form biofilms. *Eur. J. Clin. Microbiol. Infect. Dis.* **2014**, *33*, 499.

(2) Vanhée, T.; Poncelet, J.; Cheikh-Ali, S.; Bottenberg, P. Prevalence,Caries, Dental Anxiety and Quality of Life in Children with MIH in Brussels, Belgium. *J. Clin. Med.* **2022**, *11*, 3065.

(3) Margolis, H. C.; Moreno, E. C. Composition of pooled plaque fluid from caries-free and caries-positive individuals following sucrose exposure. *J. Dent. Res.* **1992**, *71*, 1776.

(4) Signorini, L.; Ballini, A.; Arrigoni, R.; De Leonardis, F.; Saini, R.; Cantore, S.; De Vito, D.; Coscia, M. F.; Dipalma, G.; Santacroce, L.; et al. Evaluation of a Nutraceutical Product with Probiotics, Vitamin D, Plus Banaba Leaf Extracts (Lagerstroemia speciosa) in Glycemic Control. *Endocr. Metab. Immune Disord.: Drug Targets* **2021**, *21*, 1356.

(5) Aoba, T. Solubility properties of human tooth mineral and pathogenesis of dental caries. *Oral Dis.* **2004**, *10*, 249.

(6) Lamont, R. J.; Koo, H.; Hajishengallis, G. The oral microbiota: dynamic communities and host interactions. *Nat. Rev. Microbiol.* **2018**, *16*, 745.

(7) Krol, D. M.; Whelan, K. Maintaining and Improving the Oral Health of Young Children. *J. Pediatr.* **2023**, *151* (1), No. e2022060417.

(8) Bardow, A.; Hofer, E.; Nyvad, B.; ten Cate, J. M.; Kirkeby, S.; Moe, D.; Nauntofte, B. Effect of saliva composition on experimental root caries. *Caries Res.* **2005**, *39*, 71.

(9) Schatz, A.; Martin, J. J.; Fosdick, L. S.; Leicester, H. M. The proteolysis-chelation theory of dental caries. *J. Am. Dent. Assoc.* **1962**, *65*, 368.

(10) Plasschaert, A. J.; Mörch, T.; König, K. G. Effect of sodium lactate under conditions of neutral pH on the release of calcium from the enamel surface *in vitro*. *Caries Res.* **1972**, *6*, 334.

(11) Williams, J. E. Relationship of sialic acid to dental caries. *J. Dent. Res.* **1967**, *46* (3), 514−521.

(12) Li, L.; Khong, M. L.; Lui, E. L. H.; Mebarek, S.; Magne, D.; Buchet, R.; Tanner, J. A. Long-chain polyphosphate in osteoblast matrix vesicles: Enrichment and inhibition of mineralization. *Biochim. Biophys. Acta, Gen. Subj.* **2019**, *1863*, 199.

(13) Candon, H. L.; Allan, B. J.; Fraley, C. D.; Gaynor, E. C. Polyphosphate kinase 1 is a pathogenesis determinant in Campylobacter jejuni. *J. Bacteriol.* **2007**, *189*, 8099.

(14) Kim, K. S.; Rao, N. N.; Fraley, C. D.; Kornberg, A. Inorganic polyphosphate is essential for long-term survival and virulence factors in Shigella and *Salmonella* spp. *Proc. Natl. Acad. Sci. U. S. A.* **2002**, *99*, 7675.

(15) Rashid, M. H.; Rumbaugh, K.; Passador, L.; Davies, D. G.; Hamood, A. N.; Iglewski, B. H.; Kornberg, A. Polyphosphate kinase is essential for biofilm development, quorum sensing, and virulence of Pseudomonas aeruginosa. *Proc. Natl. Acad. Sci. U. S. A.* **2000**, *97*, 9636.

(16) Chen, W.; Palmer, R. J.; Kuramitsu, H. K. Role of polyphosphate kinase in biofilm formation by Porphyromonas gingivalis. *Infect. Immun.* **2002**, *70*, 4708.

(17) Silby, M. W.; Nicoll, J. S.; Levy, S. B. Requirement of polyphosphate by Pseudomonas fluorescens Pf0−1 for competitive fitness and heat tolerance in laboratory media and sterile soil. *Environ. Microbiol.* **2009**, *75*, 3872.

(18) Schröder, H. C.; Neufurth, M.; Zhou, H.; Wang, S.; Wang, X.; Müller, W. E. G. Inorganic Polyphosphate: Coacervate Formation and Functional Significance in Nanomedical Applications. *Int. J. Nanomed.* **2022**, *17*, 5825.

(19) Rao, N. N.; Liu, S.; Kornberg, A. Inorganic polyphosphate in *Escherichia coli*: the phosphate regulon and the stringent response. *J. Bacteriol.* **1998**, *180*, 2186.

(20) Brown, M. R.; Kornberg, A. The long and short of it - polyphosphate, PPK and bacterial survival. *Trends Biochem. Sci.* **2008**, *33*, 284.

(21) Martin, P.; Van Mooy, B. A. Fluorometric quantification of polyphosphate in environmental plankton samples: extraction

protocols, matrix effects, and nucleic acid interference. *Appl. Environ. Microbiol.* **2013**, *79*, 273.
(22) Müller, W. E. G.; Neufurth, M.; Wang, S.; Schröder, H. C.; Wang, X. Polyphosphate Nanoparticles: Balancing Energy Requirements in Tissue Regeneration Processes. *Small* **2024**, *20*, No. e2309528.
(23) Müller, W. E. G.; Wang, S.; Neufurth, M.; Kokkinopoulou, M.; Feng, Q.; Schröder, H. C.; Wang, X. Polyphosphate as a donor of high-energy phosphate for the synthesis of ADP and ATP. *J. Cell Sci.* **2017**, *130*, 2747.
(24) Müller, W. E. G.; Schröder, H. C.; Wang, X. Inorganic Polyphosphates As Storage for and Generator of Metabolic Energy in the Extracellular Matrix. *Chem. Rev.* **2019**, *119*, 12337.
(25) Alcántara, C.; Blasco, A.; Zúñiga, M.; Monedero, V. Accumulation of polyphosphate in Lactobacillus spp. and its involvement in stress resistance. *Appl. Environ. Microbiol.* **2014**, *80*, 1650.
(26) Breiland, A. A.; Flood, B. E.; Nikrad, J.; Bakarich, J.; Husman, M.; Rhee, T.; Jones, R. S.; Bailey, J. V.; McBain, A. J. Polyphosphate-Accumulating Bacteria: Potential Contributors to Mineral Dissolution in the Oral Cavity. *Appl. Environ. Microbiol.* **2018**, *84* (7), No. e02440.
(27) Jablonski-Momeni, A.; Müller, M.; Korbmacher-Steiner, H.; Bottenberg, P. Ability of a Blue Hemoglobin-Based Liquid as a Novel Technology to Stain Initial Enamel Demineralization: A Proof-of-Concept *in vitro* Study. *Caries Res.* **2023**, *56*, 555.
(28) Alvarez-Rivera, G.; Dagnac, T.; Lores, M.; Garcia-Jares, C.; Sanchez-Prado, L.; Lamas, J. P.; Llompart, M. Determination of isothiazolinone preservatives in cosmetics and household products by matrix solid-phase dispersion followed by high-performance liquid chromatography-tandem mass spectrometry. *J. Chromatogr. A* **2012**, *1270*, 41.
(29) Daulisio, M. D. C. Z.; Schneider, R. P. Inactivation of Pseudomonas aeruginosa MDC by isothiazolones and biocide stabilizing agents. *Int. Biodeterior. Biodegrad.* **2020**, *155*, 105090.
(30) Bailey, R. T.; Holt, C. Fourier transform infrared spectroscopy and characterisation of biological calcium phosphates. In *Calcified Tissue*, Topics in Molecular and Structural Biology, Hukins, D. W. L. ed.; Macmillan Education UK: Palgrave, London, 1989. DOI: 10.1007/978-1-349-09868-2_5.
(31) Tijssen, J. P.F.; Beekes, H. W.; Van Steveninck, J. Localization of polyphosphates in Saccharomyces fragilis, as revealed by 4',6-diamidino-2-phenylindole fluorescence. *Biochim. Biophys. Acta, Mol. Cell Res.* **1982**, *721*, 394−398.
(32) Wu, D.; Yang, J.; Li, J.; Chen, L.; Tang, B.; Chen, X.; Wu, W.; Li, J. Hydroxyapatite-anchored dendrimer for in situ remineralization of human tooth enamel. *Biomaterials* **2013**, *34*, 5036.
(33) Gron, P. The state of calcium and inorganic orthophosphate in human saliva. *Arch. Oral Biol.* **1973**, *18*, 1365.
(34) Ennever, J.; Creamer, H. Microbiologic calcification: bone mineral and bacteria. *Calcif. Tissue Int.* **1967**, *1*, 87.
(35) Hoac, B.; Kiffer-Moreira, T.; Millán, J. L.; McKee, M. D. Polyphosphates inhibit extracellular matrix mineralization in MC3T3-E1 osteoblast cultures. *Bone* **2013**, *53*, 478.
(36) Francis, M. D. The inhibition of calcium hydroxypatite crystal growth by polyphosphonates and polyphosphates. *Calcif. Tissue Res.* **1969**, *3*, 151.
(37) Fogh-Andersen, N. Albumin/calcium association at different pH, as determined by potentiometry. *Clin. Chem.* **1977**, *23* (11), 2122.
(38) Abou Neel, E. A.; Aljabo, A.; Strange, A.; Ibrahim, S.; Coathup, M.; Young, A. M.; Bozec, L.; Mudera, V. Demineralization-remineralization dynamics in teeth and bone. *Int. J. Nanomed.* **2016**, *11*, 4743.
(39) Zhu, Y.; Wang, Y.; Zhang, S.; Li, J.; Li, X.; Ying, Y.; Yuan, J.; Chen, K.; Deng, S.; Wang, Q. Association of polymicrobial interactions with dental caries development and prevention. *Front. Microbiol.* **2023**, *14*, 1162380.
(40) Denucci, G. C.; Mantilla, T. F.; Amaral, F.; Basting, R. T.; França, F.; Turssi, C. P. Saliva with reduced calcium and phosphorous concentrations: Effect on erosion dental lesions. *Oral Dis.* **2018**, *24*, 957.
(41) Yilmaz, B.; Pazarceviren, A. E.; Tezcaner, A.; Evis, Z. Historical development of simulated body fluids used in biomedical applications: A review. *Microchem. J.* **2020**, *155*, 104713.
(42) Cheng, Y.; Ru, J.; Feng, C.; Liu, X.; Zeng, H.; Tan, S.; Chen, X.; Chen, F.; Lu, B.-Q. Inorganic Pyrophosphate at Serum Concentration May Not Be Able to Inhibit Mineralization: A Study in Aqueous Solutions and Serum. *ACS Omega* **2024**, *9*, 17334.
(43) Jiang, S.; Cao, Y.; Li, S.; Pang, Y.; Sun, Z. Dual function of poly(acrylic acid) on controlling amorphous mediated hydroxyapatite crystallization. *J. Cryst. Growth* **2021**, *557*, 125991.
(44) Martin, X.; Smith, L. H.; Werness, P. G. Calcium oxalate dihydrate formation in urine. *Kidney Int.* **1984**, *25*, 948.
(45) Müller, W. E. G.; Neufurth, M.; Ushijima, H.; Muñoz-Espí, R.; Müller, L. K.; Wang, S.; Schröder, H. C.; Wang, X. Molecular and biochemical approach for understanding the transition of amorphous to crystalline calcium phosphate deposits in human teeth. *Dent. Mater.* **2022**, *38*, 2014.
(46) Francis, M. D. The inhibition of calcium hydroxypatite crystal growth by polyphosphonates and polyphosphates. *Calcif. Tissue Int.* **1969**, *3*, 151.
(47) Ma, Y. X.; Hoff, S. E.; Huang, X. Q.; Liu, J.; Wan, Q. Q.; Song, Q.; Gu, J. T.; Heinz, H.; Tay, F. R.; Niu, L. N. Involvement of prenucleation clusters in calcium phosphate mineralization of collagen. *Acta Biomater.* **2021**, *120*, 213.
(48) Yang, X.; Wang, M.; Yang, Y.; Cui, B.; Xu, Z.; Yang, X. Physical origin underlying the prenucleation-cluster-mediated nonclassical nucleation pathways for calcium phosphate. *Phys. Chem. Chem. Phys.* **2019**, *21*, 14530.

https://doi.org/10.1021/acsomega.4c09093
ACS Omega 2025, 10, 10162−10172